Journal of Structural Geology, Vol. 13, No. 5, pp. 579 to 586, 1991
Printed in Great Britain

0191-8141/91 $03.00+0.00

Timing and temperature of cataclastic deformation along segments of the Towaliga fault zone, western Georgia, U.S.A.

HASSAN A. BABAIE

Department of Geology, Georgia State University, Atlanta, GA 30303, U.S.A.

JAFAR HADIZADEH

Department of Geology, University of Louisville, Louisville, KY 40292, U.S.A.

ABDOLALI BABAEI

Department of Geological Sciences, Cleveland State University, Cleveland, OH 44115, U.S.A.

and

A. MOHAMMAD GHAZI

Geology Department, University of Nebraska-Lincoln, Lincoln, NE 68588-0340, U.S.A.

(*Received* 16 *May* 1990; *accepted in revised form* 19 *October* 1990)

Abstract—Foliated cataclasite and breccia exposed along a segment of the Towaliga fault zone (TFZ) in western Georgia, U.S.A., formed during two episodes of cataclastic deformation. Conventional K–Ar crystallization ages of muscovite collected along fractures in the foliated cataclasite at Dixon Mountain, suggest that following mylonitization, at about 296 Ma (Pennsylvanian), rocks along the TFZ were elevated upward across the 300°C isothermal surface and ductile deformation via cataclastic flow was initiated. Fluid inclusion microthermometry and quartz microfabric in the cataclasite suggest that the temperature during this first cataclastic deformation, which probably occurred at a depth greater than 8 km, was between 140 and 300°C. At around 237 Ma (Late Permian), cataclastic deformation was dominated by brecciation and extensive vein sealing and formed the silicified breccias at Dixon Mountain. Muscovites from another cataclastic segment of the TFZ give a relatively low apparent age of around 269 Ma, probably because of loss of argon or mixing with younger neocrystallized muscovite during cataclasis.

INTRODUCTION

THE TOWALIGA fault zone (TFZ) at the northwestern boundary of the Pine Mountain window (PMW) in Georgia (Fig. 1) and Alabama, exposes syn-metamorphic, polydeformed mylonitic rocks (Holland 1981, Hooper & Hatcher 1988, Steltenpohl 1988). Silicifed breccia, exposed along a few segments of the TFZ (Schamel & Bauer 1980, Schamel *et al.* 1980, Kish *et al.* 1985) are interpreted to represent post-metamorphic brittle normal faults on the basis of large-scale apparent displacement of the Piedmont relative to the PMW (Schamel & Bauer 1980, Sears & Cook 1984, Higgins *et al.* 1988). The brittle faults, although locally parallel to the trace of the mylonite zones, are apparently not the products of reactivation of the older mylonitic shear zone (Schamel & Bauer 1980).

Although some of the breccias overprint the mylonitic fabric and contain clasts of mylonite (Hadizadeh *et al.* 1989, 1991), the temporal and spatial relationships between mylonitization and cataclasis along the TFZ have not yet been established. The extent and number of cataclastic deformations and whether any of these deformations produced foliated cataclasite in addition to the breccia, were previously unknown. Other problems involved the timing of the cataclastic deformation(s), the prevailing mechanism and thermal conditions, and whether the Alleghanian orogeny (Dallmeyer *et al.* 1986, Secor *et al.* 1986) included part or all of the cataclastic deformations. The objectives of this study were to understand the timing and dominant mechanisms of cataclastic deformation along portions of the TFZ, by interpreting new microstructural and microthermometric fluid inclusion data and conventional K–Ar muscovite ages of the cataclastic rocks. Our analysis helps to better reconstruct the deformation history of the TFZ.

Throughout this paper we use the classification of fault rocks by Sibson (1977). We stress the distinction between ductile deformation by crystal-plastic mechanisms (ductile–plastic) vs ductile deformation by cataclastic flow (ductile–brittle) (Rutter 1986).

GEOLOGIC BACKGROUND

The PMW in the Georgia and Alabama Piedmont exposes Grenville-age basement and its unconformable cover of Pine Mountain Group (Odom *et al.* 1973, Schamel & Bauer 1980, Hatcher 1984, Sears & Cook 1984, Higgins *et al.* 1988). The overall structure of the PMW has been interpreted as NW-vergent, nearly recumbent thrust nappes, arched about gently NE-plunging axes (Schamel *et al.* 1980, Sears *et al.* 1981, Hatcher 1984). Nelson *et al.* (1987), using COCORP data, suggested that a post-Alleghanian, late Paleozoic and/or Mesozoic normal fault offsets the Grenville basement by 9 km along the known trace of the TFZ.

The last mylonitization episode along the TFZ is thought to be related to the Alleghanian orogeny at about 300 Ma (Wampler *et al.* 1970, Goldberg & Steltenpohl 1988, Kish 1988), when the fault cooled below the 300°C (Cliff 1985) blocking temperature for biotite (Kish *et al.* 1985). 190 Ma old diabase dikes (Ragland *et al.* 1983) that cut across the fault provide a minimum age for the TFZ (Schamel & Bauer 1980). However, Reinhardt *et al.* (1984) proposed that the latest brittle phase of deformation along the TFZ may be as young as Paleocene.

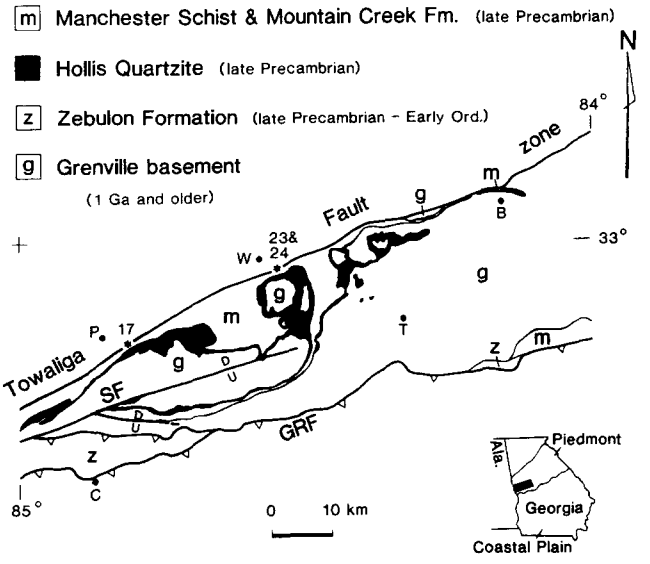

Fig. 1. Geologic map of part of the Pine Mountain window in Georgia showing SE boundary of Towaliga fault zone, sample locations (shown by *), and study area (filled rectangle) (modified from Higgins *et al.* 1988). Dixon Mountain is at TF23 and TF24 (TF omitted on map), south of Woodbury (W) (Woodbury 7.5 minute Quadrangle). TF17 is a roadcut on the Mountain Top road about 0.5 mile off highway 190 at Hines Gap (Pine Mountain 7.5 minute Quadrangle). Grenville basement includes Sparks Schist. P = Pine Mountain, B = Barnesville, T = Thomaston, C = Cataula, SF = Shiloh fault, GRF = Goat Rock fault.

CATACLASTIC MICROFABRICS

Cataclastic deformation in the TFZ has generated breccia (Grant 1967, Davis 1980, Kish *et al.* 1985), and foliated cataclasite (Hadizadeh & Babaie 1988, Babaie *et al.* 1989). Due to widespread silicification, breccia is better preserved than the highly fractured, non-silicified cataclasites, and occurs as relatively small, *ca* 600 × 200 m oval ridges such as Dixon Mountain (Fig. 1), that have 100–200 m of relief above the surrounding valleys. The occurrence of bodies of silicified breccia has been reported in areas up to 120 km northeast of the study area along the approximate trend of the Towaliga fault zone (Davis 1980). Generally, fragments within the matrix of silicified breccia are of two distinct types: (1) crushed vein-quartz with little sign of plastic strain (Fig. 2a); and (2) composite clasts bearing evidence of older, more widespread deformation, both mylonitic and cataclastic (Fig. 2b). At Dixon Mountain, some of the composite clasts show a flow-like structure composed of dark bands of very fine (5–10 μm) to sub-micron angular quartz grains (Fig. 2b). Under plane-polarized light the bands exhibit a fabric with fluxion structure. Fine-grained and cryptocrystalline quartz crystals make up the silicic matrix that gives the breccia coherence. Silicification obliterated most of the pre-existing mylonitic and cataclastic fabric. Numerous boxwork quartz veins cut across each other and the breccia (Fig. 2c). Veins generally have a thickness of less than 1 mm, but cm-thick veins are also common in the breccias, in which crystals are very coarse (1–2 cm) and form the so-called dog-tooth structure. Clasts of vein material are distinguished from clasts of cataclasite by their euhedral crystal shapes and uniform extinction reflecting their less deformed structure. The crystal faces of vein-quartz are marked by dark solid inclusions that accentuate accreted growth layers.

Sparse, thin zones of microbreccia occur within the isotropic silicified breccias, cut across quartz veins, and show multiple crack–seal and brecciation episodes. The microbreccia zones range in thickness between a fraction of a millimeter and a few millimeters. Grain size in the microbreccia zones ranges between 5 μm (and probably smaller) and 1 mm and decreases progressively toward the middle of the zone.

Foliated cataclasites form thin bodies at the margins of the silicified breccias. The foliation in the cataclasite is defined by mm-scale, anastomosing shear fractures, that enclose slivers of single or aggregate quartz crystals. Quartz slivers show a preferred orientation and thin bands of cataclasite are parallel to a pervasive set of intergranular shear fractures between fragments (Fig. 2d). Fragments in the cataclasite display patchy extinction, suggestive of submicroscopic intragranular fracturing and rotation (Tullis & Yund 1987). Transgranular fractures are oblique to the major intergranular fractures which define the foliation (Fig. 2d).

Scarce microstructures indicative of grain boundary migration recrystallization (Guillope & Poirier 1979, Urai *et al.* 1986) occur in the foliated cataclasites. The exclusive occurrence of the recrystallized grains inside mylonitic fragments, and the fact that these microstructures are cut by shear fractures in the cataclasite, suggest that the recrystallized grains are the products of crystal-plastic deformation during an earlier mylonitization

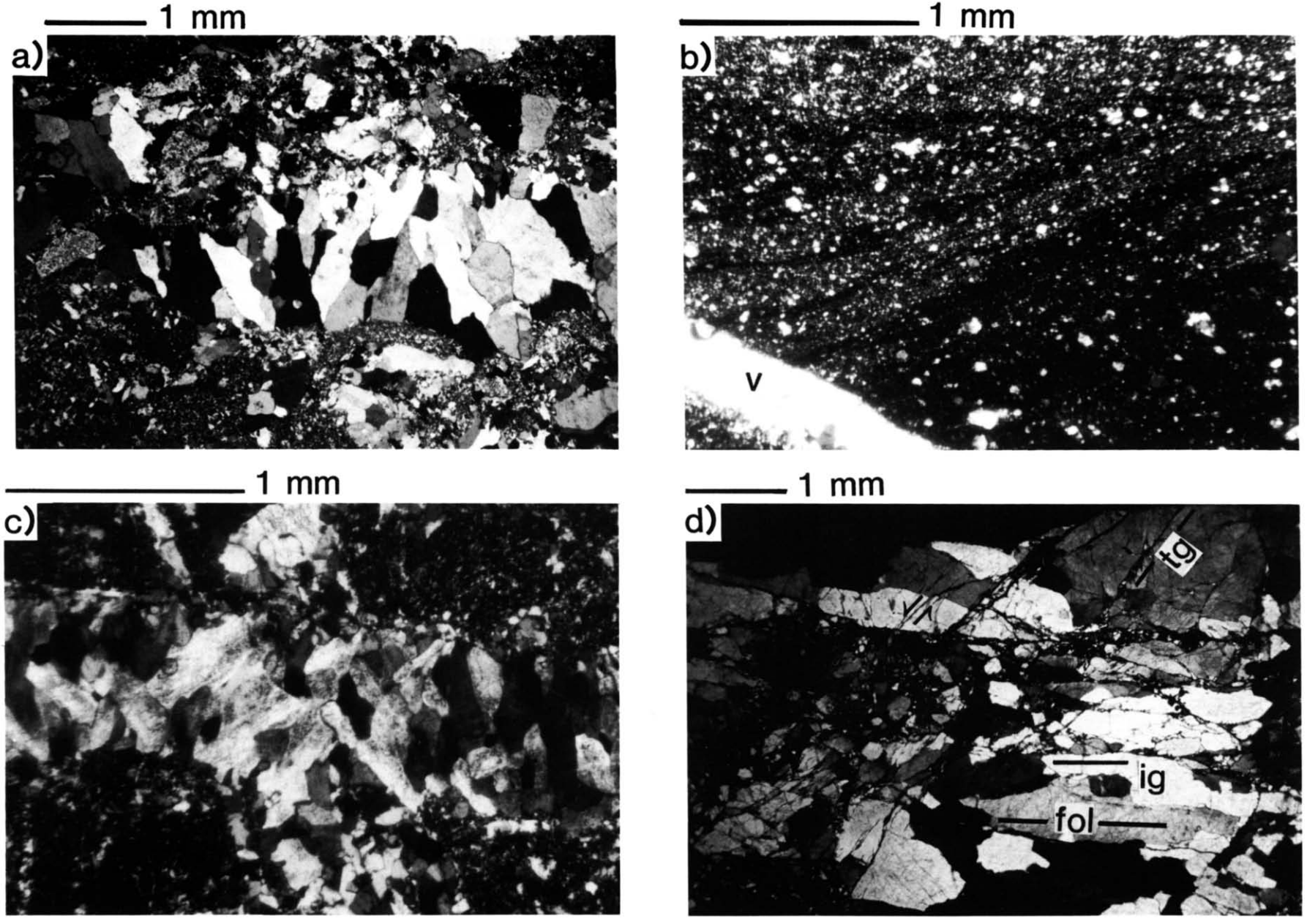

Fig. 2. (a) Clast of quartz vein material in the breccia enclosed by smaller clasts of quartz and crystals of cryptocrystalline quartz (matrix); (b) clast of ultracataclasite in the breccia with fluxion structure (apparent under plane polarized light). Under higher magnification, the small grains in the clast are angular and enclosed by a submicron matrix. 'V' is quartz vein cutting the clast; (c) massive boxwork vein system in the breccia. Veins are cutting across each other and the matrix made of cryptocrystalline quartz crystals; (d) fracture-dominated microstructure of the foliated cataclasite. Intergranular (ig) and transgranular (tg) shear fractures (arrows show sense of shear) break the quartzitic rock into elongate slivers with longest dimension parallel to the cataclastic foliation (fol), gouge zones and intergranular fractures.

event. Microscopically, no evidence for quartz recrystallization is apparent along the fractures.

ESTIMATES OF TEMPERATURE AND AGE OF CATACLASTIC DEFORMATION

Quartz crystals in veins and adjacent grains in the foliated cataclasites were analyzed for fluid generations and compositions in fluid inclusions. Fluid inclusion analysis was conducted on a modified USGS-type heating and freezing stage mounted on a Zeiss WL microscope. Different parts of doubly-polished samples were frozen to observe the behavior of the entrapped material and to estimate the total salinity as equivalent wt% NaCl from ice-melting temperatures. Homogenization temperatures of the inclusions were determined on the same inclusions.

The fluid inclusions contain liquid and water vapor. Trails of inclusions form arrays that cross each other and grain boundaries, indicating that they are secondary and formed when fluids healed fractures. The sizes of the generally irregular inclusions range between 2 and 50 μm. The ice-melting temperatures range between -0.7 and 0°C (Table 1), indicating salinities of 0–1.2 wt% NaCl equivalent (almost fresh water) (Roedder 1984).

The homogenization temperatures have a narrow range between 141 and 175°C with a mean of 159°C (Table 1). Using the 1% NaCl equivalent curves of Potter (1977), and assuming that brittle deformation of quartz occurred below 300°C (Voll 1976), pressure corrections needed for estimation of the trapping temperature (T_t) were made over a depth range of 1–8 km (Table 2). The maximum depth below which T_t would exceed the 300°C limit is, under lithostatic pressure conditions, between 7 and 8 km (Table 2). However, a calculated 319°C for mean T_t at a depth of 8 km (Table 2) requires a geothermal gradient of 40°C km^{-1}. The maximum depth could be significantly greater in the likely case of effective pressure being less than lithostatic pressure or if the pressure gradient were less than the 25 MPa km^{-1} used in our calculations (Table 2). For example, if the effective pressure where the fluid inclusions formed were half the lithostatic pressure, the mean T_t would stay below 300°C down to 14 km. We suggest therefore that veins formed at depths greater than 8 km unless the geothermal gradient exceeded 40°C km^{-1} or the silica-rich fluids originated from a hot source.

X-ray diffraction patterns of micas from breccia (TF24 and TF17) and foliated cataclasites (TF23, Fig. 1) indicate that they are muscovite. At Dixon Mountain (TF23 and TF24), flakes of this muscovite are commonly microfaulted, locally buckled due to shear along fractures, and show no evidence of overgrowth. Muscovite is in places altered to chlorite along fracture planes. The Dixon Mountain muscovites occur almost exclusively along fractures and have non-sigmoidal shapes. At station TF17, where ultramylonites are brecciated (Hadizadeh *et al.* 1991) muscovites occur as subhedral grains in the matrix (mainly along interclast fractures), and as mica fish (Lister & Snoke 1984) within mylonitic fragments. The interclast muscovites have variable sizes compared to the intraclast mica fish which are finer grained and have a more uniform size. The tails of the sigmoidal muscovite fish in the mylonitic clasts are parallel to the mylonitic foliation which is defined by the

Table 1. Thirty homogenization temperatures (T_h) of fluid inclusions in 19 grains (g) near veins, and 11 veins (v) in foliated cataclasite at station TF23. Data are given in a histogram form. Ice melting temperatures are given in parentheses. T'_h and SD are mean and standard deviation of the homogenization temperatures; n.d. = not determined

	Homogenization temperature (T_h) (°C)			
n	140	150	160	170
1	141.1 (−0.5)g	150.0 (−0.2)g	160.1 (−0.4)g	170.5 (−0.2)g
2	147.0 (−0.5)g	150.0 (−0.2)g	160.2 (−0.2)g	170.7 (n.d.)g
3	149.0 (−0.3)v	150.8 (−0.4)v	163.4 (−0.3)v	171.5 (−0.2)g
4	149.9 (−0.4)g	152.0 (0.0)g	165.5 (−0.2)v	174.9 (n.d.)v
5	149.9 (−0.3)g	152.7 (n.d.)g	165.8 (−0.5)v	175.0 (n.d.)g
6		155.0 (−0.2)g	168.6 (−0.3)g	
7		155.4 (−0.2)v	168.6 (−0.3)v	
8		155.7 (n.d.)v		
9		156.8 (−0.4)g		
10		156.9 (−0.2)v		
11		157.5 (−0.7)v		
12		157.6 (0.0)g		
13		158.5 (−0.2)g		
		(mean = 159)		

	Grains (°C)	Veins (°C)	All (°C)
T'_h	157.70	160.3	158.70
SD	9.57	7.94	8.95

alignment of quartz ribbons and recrystallized tails of sigmoidal feldspars, suggesting that the intraclast micas recrystallized during mylonitization.

Conventional K–Ar analysis (Dalrymple & Lanphere 1969) was applied to determine the ages of three samples of muscovite extracted from fractures in the breccias and foliated cataclasites. Sample TF24 (Fig. 1) has the youngest muscovite apparent age of 237 Ma (Late Permian) (Table 3) and is from a coarse-grained breccia at Dixon Mountain with extensive veining and abundant cm-sized clasts of vein-quartz. Sample TF23 (Fig. 1) gives the oldest apparent age of 296 Ma (Pennsylvanian) and is from the foliated cataclasites surrounding the breccias at Dixon Mountain. TF17 (Fig. 1), collected from brecciated quartz-ribbon ultramylonites near Pine Mountain town (Hadizadeh *et al.* 1991), yields an apparent age of 269 Ma (Early Permian).

DISCUSSION

Massive silicification, boxwork and open-vein quartz crystallization, and fluid inclusion data, indicate that the breccia developed in a brittle regime of probable extensional nature in which dilute (0–1.2 wt% salts) hydrothermal fluids were present. While the fine grain-size and fluxion structure in some of the clasts suggest a mylonitic origin, the lack of an obvious crystallographic preferred orientation (interpreted by using a quartz plate) and the fragmental texture discernible under plane polarized light, suggest that the clasts are ultracataclasite. Grains coarser than the 5 μm were distinguished as cataclastic from their angular to subangular shapes and their enclosing matrix. However, some finer grains (beyond the resolution of the microscope) in the foliated cataclasite may be products of recrystallization. The similarity between textures produced in experimental cataclastic deformation (Logan *et al.* 1979, Chester *et al.* 1985, Shimamoto 1989) and textures in the studied samples suggests that cataclastic flow was the dominant deformation mechanism in the foliated cataclasites of the TFZ. It has been shown that cataclastic flow can produce both foliation and fluxion structure at different scales (Chester *et al.* 1985). The foliated ultracataclasite fragments in the breccia (Fig. 2b) indicate either that the breccia zone increased in thickness as it developed, or that the foliated rocks formed in narrow bands within a breccia zone of fixed thickness and were later rebrecciated.

Cataclastic deformation involves infiltration of fluids and significant changes in porosity and permeability (Stel 1986, Hirth & Tullis 1989). These processes can result in the loss or gain of argon in muscovite, thereby complicating interpretation of the K–Ar ages. The dated muscovites are either relict grains from mylonitization or they crystallized during the later cataclastic deformation. The occurrence of broken and microfaulted muscovite grains almost exclusively along intergranular fractures and cataclastic bands strongly suggests that the micas in TF23 and TF24 and those which occur along fractures in TF17 were formed synchronously with cataclastic deformation and are not relict grains recrys-

Table 2. Trapping temperature (T_t) range for fluid inclusions in grains and veins of foliated cataclasites (see Table 1), using the 1% NaCl equivalent curves of Potter (1977) for pressure correction ($T_t = T_h$ + correction). The pressure gradient (lithostatic) was assumed to be 25 MPa km^{-1} for a quartzo-feldspathic crust.* Homogenization temperature (T_h) range and mean homogenization temperature taken from Table 1

	Correction for T_h			Trapping temperature (T_t)		
Depth (km)	minimum (141°C)	maximum (175°C)	mean (159°C)	minimum (°C)	maximum (°C)	mean (°C)
1	28	23	25	169	193	184
2	46	40	42	187	210	201
3	65	60	62	206	230	221
4	85	80	82	226	250	241
5	105	98	103	246	268	262
6	120	117	120	261	287	279
7	142	140	140	283	310	299
8	160	155	160	301	330	319

*The corrections will be less at all depths if pressure was effective pressure. Therefore, the depth above which T_t will remain below 300°C will increase. See text for explanation.

Table 3. Conventional K–Ar apparent crystallization ages of muscovite of the foliated cataclasite (TF23) and breccia (TF24) at Dixon Mountain, and apparent cooling age of muscovite in brecciated ultramylonites near the town of Pine Mountain (TF17)

		Potassium		Radiogenic argon			Apparent age	
Sample	Mass (g)	(%)	±	(%)	(pmol g^{-1})	±	(Ma)	±
TF17	0.0281	4.301	0.043	87.9	2158.77	33.24	268.5	4.6
TF23	0.0268	4.803	0.048	96.6	2675.44	38.55	295.6	4.8
TF24	0.0473	6.359	0.064	84.2	2786.40	44.40	236.5	4.2

tallized during an earlier mylonitization event. The presence of mica fish in the ultramylonite clasts in the breccia of station TF17 suggests that at least some of the dated muscovites are relict and of mylonitic origin. Brittle fracture of quartz in the foliated cataclasites and breccias suggests that muscovite crystallized below 300°C (Voll 1976). Therefore, the conventional K–Ar muscovite ages most likely represent the time of crystallization during cataclastic deformation rather than cooling ages, except for sample TF17. The 269 Ma apparent age of muscovite at TF17 is less than the published cooling age of 300 Ma for mylonites along other segments of the Towaliga fault zone (Wampler *et al.* 1970, Goldberg & Steltenpohl 1988, Kish 1988), probably as a result of argon loss and/or formation of new muscovite during cataclastic deformation (along fractures) which may have mixed with older muscovite during sampling. The almost 60 Ma difference between the apparent ages of the foliated cataclasite (TF23) and breccia (TF24) at Dixon Mountain (Table 3) could be due to the loss and/or gain of argon during cataclasis. However, the occurrence of clasts of ultracataclasite in the breccia suggests that the breccia is younger. Thus, the 237 Ma muscovite crystallization age in the breccia may document a different episode of cataclastic deformation from the one during which the foliated cataclasite was formed.

Our muscovite age data suggest that the ductile–plastic deformation which produced mylonites at least 300 Ma ago (Wampler *et al.* 1970, Goldberg & Steltenpohl 1988, Kish 1988) was followed by ductile–brittle deformation accommodated by cataclastic flow at around 296 Ma (Pennsylvanian) when foliated cataclasites (TF23) and ultracataclasites around Dixon Mountain were developed. This episode, which most probably took place at a temperature below 300°C as suggested by quartz microfabric, was restricted to narrow zones surrounding relatively undeformed pods of quartzitic rocks. Our unpublished data (using Riedel shears) and work by Hadizadeh *et al.* (1991) show that the kinematics of this cataclastic deformation are consistent with right-lateral displacement during mylonitization (Steltenpohl 1988, Hooper & Hatcher 1989). This implies that the proposed normal faulting (Schamel & Bauer 1980, Nelson *et al.* 1987) did not occur during the first cataclastic episode at 296 Ma. A second episode, documented in the silicified breccias of Dixon Mountain, probably occurred around 237 Ma (Late Permian), or possibly earlier if there has been argon loss. This episode involved intermittent brecciation of surrounding undeformed rocks and earlier cataclasites, veining, and neomineralization of mica and quartz by hydrothermal fluids.

CONCLUSIONS

At least two episodes of cataclastic deformation occurred in the breccia and cataclasites of the TFZ. Muscovite crystallization ages show that foliated cataclasites at Dixon Mountain formed by cataclastic flow at about 296 Ma (during the Alleghanian orogeny) and later brecciated at around 237 Ma. Our data suggest that a transition from predominantly crystal-plastic deformation to microscopic brittle deformation occurred at around 300 Ma along the TFZ. Locally (at TF17), muscovites in the breccia give an underestimate of the cooling age of mylonitization along the TFZ probably due to argon loss during cataclasis and/or mixing of younger neomineralized muscovite formed during cataclasis with relict mylonitic muscovite. The proposed normal faulting along the TFZ (Nelson *et al.* 1987) is younger than the 296 Ma foliated cataclasites.

Application of conventional K–Ar dating in cataclastic rocks is complicated by the loss and/or gain of argon due to fracturing and fluid activity. However, a careful study of clast composition and fabric and cross-cutting relationships in cataclastic rocks can help to interpret the ages more accurately.

Acknowledgements—We thank Marion Wampler and Dave Vanko for allowing us to use their K–Ar and fluid inclusion labs, respectively. We are grateful to Carol Simpson, Rick Groshong, Stephen Kish, Mark Steltenpohl, Steven Schamel, Dave Vanko, Judy Kreps and two anonymous reviewers for their critical review which led to improvement of the manuscript. Acknowledgment is made to the Donors of The Petroleum Research Fund, administered by the American Chemical Society, for support of this research granted to H. A. Babaie.

REFERENCES

Babaie, H. A., Hadizadeh, J. & Babaei, A. A. 1989. Fluid inclusion study of foliated cataclasites along the Towaliga fault zone, west central Georgia (abstract). *Geol. Soc. Am. Abs. w. Prog.* **21**, A65.

Chester, F. A., Friedman, M. & Logan, J. M. 1985. Foliated cataclasites. *Tectonophysics* **111**, 139–146.

Cliff, R. A. 1985. Isotopic dating in metamorphic belts. *J. geol. Soc. Lond.* **142**, 97–110.

Dallmeyer, R. D., Wright, J. E., Secor, D. T. & Snoke, A. W. 1986. Character of the Alleghanian orogeny in the southern Appalachians: Part II. Geochronological constraints on the tectonothermal evolution of the eastern Piedmont in South Carolina. *Bull. geol. Soc. Am.* **97**, 1329–1344.

Dalrymple, G. B. & Lanphere, M. A. 1969. *Potassium–Argon Dating*. W. H. Freeman, San Francisco.

Davis, G. J. 1980. The southwestern extension of the Middleton–Lowndesville cataclastic zone in the Greensboro, Georgia, area and its regional implications. Unpublished M.S. thesis, University of Georgia, Athens, Georgia, U.S.A.

Goldberg, S. A. & Steltenpohl, M. G. 1988. Evidence for Alleghanian penetrative deformation in the Inner Piedmont of Alabama (abs.). *Geol. Soc. Am. Abs. w. Prog.* **20**, 267.

Grant, W. H. 1967. Geology of the Barnesville area and Towaliga fault, Lamar County, Georgia. *Georgia geol. Soc. Field Trip Guide.*

Guillope, M. & Poirier, J. P. 1979. Dynamic recrystallization during creep of single-crystalline halite: an experimental study. *J. geophys. Res.* **84**, 5557–5567.

Hadizadeh, J. & Babaie, H. A. 1988. A microstructural study of cataclastic rocks in the Towaliga Fault zone, Pine Mountain belt, Georgia (abs.). *Geol. Soc. Am. Abs. w. Prog.* **20**, A180.

Hadizadeh, J., Babaei, A. A. & Babaie, H. A. 1989. Intermittent brittle and ductile deformation in a rectograde mylonite zone. *Geol. Soc. Am. Abs. w. Prog.* **21**, A70.

Hadizadeh, J. Babaie, H. A. & Babaei, A. A. 1991. Development of interlaced mylonites, cataclasites and breccias: example from the Towaliga fault, south central Appalachians. *J. Struct. Geol.* **13**, 63–70.

Hatcher, R. D. Jr. 1984. Southern and central Appalachian basement massifs. In: *The Grenville Event in the Appalachians and Related Topics* (edited by Bartholomew, M.). *Spec. Pap. geol. Soc. Am.* **194**, 149–160.

Higgins, M. W., Atkins, R. L., Crawford, T. J., Crawford, R. F., III,

Brooks, R. & Cook, R. B. 1988. The structure, stratigraphy, tectonostratigraphy, and evolution of the southernmost part of the Appalachian orogen. *Prof. Pap. U.S. geol. Surv.* **1475**.

Hirth, G. & Tullis, J. 1989. The effect of pressure and porosity on the micromechanics of the brittle-ductile transition in quartzite. *J. geophys. Res.* **94**, 17,825–17,838.

Holland, W. A. Jr. 1981. The kinematic and metamorphic development of the Towaliga–Goat rock mylonites, Georgia–Alabama. Unpublished Ph.D. thesis, Florida State University, Tallahassee, Florida, U.S.A.

Hooper, R. J. & Hatcher, R. D., Jr. 1988. Mylonites from the Towaliga fault zone, central Georgia: Products of heterogeneous non-coaxial deformation. *Tectonophysics* **152**, 1–17.

Kish, S. A. 1988. Post-Alleghanian uplift adjacent to major ductile fault zones in the southern Appalachian Piedmont. *Geol. Soc. Am. Abs. w. Prog., Southeast. Sect.* **20**, 274.

Kish, S. A., Hanley, T. B. & Schamel, S. 1985. Geology of the southwestern Piedmont of Georgia. *Geol. Soc. Am. Field Guidebook*, 1–8.

Lister, G. S. & Snoke, A. W. 1984. S–C mylonites. *J. Struct. Geol.* **6**, 617–638.

Logan, J. M., Friedman, M., Higgs, N., Dengo, C. & Shimamoto, T. 1979. Experimental studies of simulated gouge and their application to studies of natural fault zones. Proc. 8th conf. on Analysis of Actual Fault zones in Bedrock. *U.S. geol. Surv. Open-file Rep.* **79-1239**, 305–343.

Nelson, K. D., Arnow, J. A. & Giguere, M. 1987. Normal-fault boundary of an Appalachian basement massif?: Results of COCORP profiling across the Pine Mountain belt in western Georgia. *Geology* **15**, 832–836.

Odom, A. L., Kish, S. & Leggo, P. 1973. Extension of "Grenville Basement" to the southern extremity of the Appalachians: U–Pb ages of zircons (abs.). *Geol. Soc. Am. Abs. w. Prog.* **5**, 425.

Potter, R. W. 1977. Pressure corrections for fluid-inclusion homogenization temperatures based on the volumetric properties of the system NaCl–H_2O. *J. Res., U.S. geol. Surv.* **5**, 603–607.

Ragland, C., Hatcher, R. D., Jr. & Whittington, D. 1983. Juxtaposed Mesozoic diabase dike sets from the Carolinas: A preliminary assessment. *Geology* **11**, 394–399.

Reinhardt, J., Prowell, D. C. & Christopher, R. A. 1984. Evidence for Cenozoic tectonism in the southwest Georgia Piedmont. *Bull. geol, Soc. Am.* **95**, 1176–1187.

Roedder, E. 1984. Fluid Inclusions. In: *Reviews of Mineralogy* (edited by Ribbe, P. H.). *Miner. Soc. Am.* **12**.

Rutter, E. H. 1986. On the nomenclature of mode of failure transitions in rocks. *Tectonophysics* **122**, 381–387.

Schamel, S. & Bauer, D. T. 1980. Remobilized Grenville basement in the Pine Mountain window. In: *The Caledonides in the USA* (edited by Wones, D. R.). *Dept. Geol. Sci., Virginia Polytech. Inst. & State Univ. Mem.* **2**, 313–316.

Schamel, S., Hanley, T. B. & Sears, J. W. 1980. Geology of the Pine Mountain window and adjacent terranes in the Piedmont province of Alabama and Georgia. *Geol. Soc. Am. Southeast Sect. Guidebook*.

Sears, J. W. & Cook, R. B. 1984. An overview of the Grenville basement complex of the Pine Mountain window, Alabama and Georgia. *Spec. Pap. geol. Soc. Am.* **194**, 281–287.

Sears, J. W., Cook, R. B., Gilbert, O. E., Carrington, T. & Schamel, S. 1981. Stratigraphy and structure of the Pine Mountain window in Georgia and Alabama. *Georgia geol. Surv. Inf. Circular* **54-A**, 41–53.

Secor, D. T., Snoke, A. W., Bramlett, K. W., Costello, O. P. & Kimbrell, O. P. 1986. Character of the Alleghanian orogeny in the southern Appalachians: Part I. Alleghanian deformation in the eastern Piedmont of South Carolina. *Bull. geol. Soc. Am.* **97**, 1319–1328.

Shimamoto, T. 1989. The origin of *S–C* mylonites and a new fault-zone model. *J. Struct. Geol.* **11**, 51–64.

Sibson, R. H. 1977. Fault rocks and fault mechanisms. *J. geol. Soc. Lond.* **133**, 191–213.

Stel, H. 1986. The effect of cyclic operation of brittle and ductile deformation on metamorphic assemblage in cataclasites and mylonites. *Pure & Appl. Geophys.* **124**, 289–307.

Steltenpohl, M. G. 1988. Kinematics of the Towaliga fault, Bartletts Ferry, and Goat Rock fault zones, Alabama: the late Paleozoic dextral shear system in the southernmost Appalachians. *Geology* **16**, 852–855.

Tullis, J. & Yund, R. A. 1987. Transition from cataclastic flow to dislocation creep of feldspar: Mechanisms and microstructures. *Geology* **15**, 606–609.

Urai, J. L., Means, W. D. & Lister, G. S. 1986. Dynamic recrystallization of minerals. In: *Mineral and Rock Deformation: Laboratory Studies—The Paterson Volume* (edited by Hobbs, B. E. & Heard, H. C.). *Am. Geophys. Un. Geophys. Monogr.* **36**, 161–200.

Voll, G. 1976. Recrystallization of quartz, biotite, and feldspars from Erstfeld to the Levantina nappe, Swiss Alps, and its geological implications. *Schweiz. miner. petrogr. Mitt.* **56**, 641–647.

Wampler, J. M., Neathery, T. L. & Bentley, R. D. 1970. Age relations in the Alabama Piedmont. In: *Geology of the Brevard Fault Zone and Related Rocks of the Inner Piedmont of Alabama* (edited by Bentley, R. D. & Neathery, T. L.). *Alabama geol. Soc. Guidebook*, 81–90.